Optimization of fuel cell membrane electrode assemblies for transition metal ion-chelating ordered mesoporous carbon cathode catalysts[a]

Johanna K. Dombrovskis,[b] Cathrin Prestel, and Anders E. C. Palmqvist[b]
Department of Chemical and Biological Engineering, Applied Surface Chemistry, Chalmers University of Technology, SE-412 96 Göteborg, Sweden

(Received 22 October 2014; accepted 18 November 2014; published online 9 December 2014)

Transition metal ion-chelating ordered mesoporous carbon (TM-OMC) materials were recently shown to be efficient polymer electrolyte membrane fuel cell (PEMFC) catalysts. The structure and properties of these catalysts are largely different from conventional catalyst materials, thus rendering membrane electrode assembly (MEA) preparation parameters developed for conventional catalysts not useful for applications of TM-OMC catalysts. This necessitates development of a methodology to incorporate TM-OMC catalysts in the MEA. Here, an efficient method for MEA preparation using TM-OMC catalyst materials for PEMFC is developed including effects of catalyst/ionomer loading and catalyst/ionomer-mixing and application procedures. An optimized protocol for MEA preparation using TM-OMC catalysts is described. [http://dx.doi.org/10.1063/1.4902995]

For the last decades, fuel cells have received attention from both academia and industry as efficient and clean energy conversion devices. The major limiting factor for their large scale application is their high cost, mainly due to the costly platinum used to catalyze the electrochemical reactions of the fuel cell.[1] Today, two different lines of research seek to overcome this problem, the first targeting reducing the platinum content in fuel cell catalysts by improving its distribution throughout the electrode, while the second seeks to circumvent the use of platinum or other noble metals altogether. This second approach has seen major progress in the development of cathode catalysts in recent years.[2–5] The non-noble metal catalysts discussed in these publications are based on transition metal-binding organic materials. Especially, carbon-based materials containing nitrogen and iron and/or cobalt have shown encouraging results in catalyzing the oxygen reduction reaction (ORR), and a number of different approaches to synthesize such catalysts have been published recently.[1,5–12] Although apparently compositionally related, these different synthesis approaches cause differences in structures and properties of the materials prepared. Some behave rather similar to conventional carbon-black supported noble metal catalysts and can therefore be applied in membrane electrode assembly (MEA) in similar ways[13,14] or by small adjustments of conventional MEA preparation procedures.[15,16] Despite this, some of the new catalyst materials, specifically functionalized ordered mesoporous carbon (functionalized OMC) materials, are quite different from conventional catalysts in structure and properties. The use of functionalized OMC materials in cathodes for polymer electrolyte membrane fuel cells (PEMFCs) therefore requires a whole new set of optimized MEA preparation parameters. In the past non-functionalized OMCs and other nanostructured carbons were used as support materials for noble metal catalysts.[17–21] Lately, these materials have been developed further to include additional functionalization. As an effect, the materials can now act

[a]Invited for the Mesoporous Materials special topic.

[b]Authors to whom correspondence should be addressed. Electronic mail: harterj@chalmers.se and anders.palmqvist@chalmers.se

as catalyst and catalyst support simultaneously. All OMCs, including functionalized OMCs, have tunable pore walls, pore sizes, and surface areas, which are interesting both to their role as catalyst and as support material. Typically, pores are in the size range of 3–6 nm and specific surface areas in the range of 550–1000 $m^2\ g^{-1}$. Recently, several noble metal-free functionalized OMC fuel cell catalyst materials have been presented where the OMC matrix was functionalized with either nitrogen,[22,23] phosphorous,[24,25] or both nitrogen and transition metal ions.[23]

So far, the research focus regarding these functionalized OMCs has been mainly on catalyst synthesis and catalyst active site structure. However, very little on the MEA preparation procedures using catalyst materials with a functionalized OMC structure is known. In this work, an optimized procedure for MEA preparation using nitrogen- and transition metal-containing OMC catalysts at the cathode is presented. The influence of important parameters, such as catalyst loading and ionomer to catalyst ratio is described. Special consideration is given to the preparation and application procedures of the ionomer-catalyst-suspension, in the following referred to as the catalyst ink. The application procedures used to apply the catalyst ink on the gas diffusion layer (GDL) proved to be of utmost importance to the achieved overall fuel cell activity. Here, we discuss reasons for the major influence of the application procedure and specify optimized application parameters.

Catalyst preparation. A cubic Ia3d mesoporous silica powder, prepared as described by Kleitz *et al.*,[26] was used as a template to synthesize a series of nitrogen- and iron-functionalized OMCs. To prepare the functionalized OMCs, the silica was covered with 0.5 M PTSA (*p*-Toluenesulfonic acid 98% from Merck) in ethanol for 2 h, followed by vacuum filtration, washing with ethanol, and drying (2 h, 80 °C). Next, the carbon, nitrogen, and metal precursors were added in amounts corresponding to the silica pore volume (determined by nitrogen physisorption measurements, typically ∼1 cm^3/g silica). Furfurylamine (>99% from Sigma-Aldrich) was used as combined carbon and nitrogen source while $FeCl_3$ (>98% hexahydrate from Sigma-Aldrich) was used as source for iron. A mixture of 6 g of $FeCl_3$ in 10 g furfurylamine was used to impregnate the silica. This was followed by a heat treatment at 100 °C in air for 2 h and a subsequent second impregnation with the precursor solution to improve the pore filling of the silica. Next, the samples were heat treated for 2 h in air at 160 °C. The two heat treatment steps lead to polymerization of the carbon precursor. After this polymerization, the samples were pyrolized under nitrogen atmosphere in a tube furnace at 950 °C for 2 h. Heating- and cooling rates were 15 K min^{-1}, and the nitrogen flow through the tube was 100 ml min^{-1}. Finally, the silica template was removed by immersion of the powder in 40% HF (24 h) and subsequent washing and drying for 24 h at 100 °C. The resulting nitrogen- and transition metal-functionalized OMC materials (abbreviated as Fe/N-OMC) had an iron loading of 0.9 ± 0.2 wt. % according to energy dispersive X-ray spectroscopy (EDX) measurements. Unless stated otherwise, all measurements shown here were done with the same batch of Fe/N-OMC material. Further details of the catalyst synthesis are described elsewhere.[23]

Characterization of the mesoporous structure. In order to verify the ordered mesoporosity and surface conformation of the catalyst powders, high resolution scanning electron microscopy (SEM) was done using a LEO ULTRA 55 FEG instrument. Nitrogen adsorption and small angle X-ray scattering analyses were done (see supplementary material for results and experimental details[33]).

Performance evaluation in a polymer electrolyte fuel cell. Fuel cell experiments were conducted in a 2.25 cm^2 single cell fuelled with 10% H_2 in argon at the anode and with the cathode fuelled with O_2 or N_2 as a reference. In this setup, the cathode acted as working electrode, while the anode acted as both counter electrode and reference. This allows for the measurement of the whole cell voltage significant for the evaluation of MEA performance. The potentials reported here are denoted versus Reversible Hydrogen Electrode (RHE). All measured cell potentials shown here are corrected for the voltage shift due to the lower 10% partial pressure of H_2 in argon using the Nernst equation, thus allowing for comparison with fuel cells run with 100% H_2.

At the anode, a commercial gas diffusion electrode (10 wt. % Pt/C electrode from Electrochem., Inc.) with a loading of 0.5 mg Pt per cm^2 was used. At the cathode, a Toray EC-TPI-060T GDL and our catalyst powders were used. To prepare the cathode, catalyst ink made from catalyst powder and Nafion ionomer was applied on the GDL, wherein the used Nafion was from a 5 wt. % Nafion solution in lower aliphatic alcohols (Sigma-Aldrich). A NRE-117 Nafion membrane from Sigma-Aldrich was used as electrolyte. The as-received NRE-117 membranes were boiled for 1 h

in 3% hydrogen peroxide solution (diluted from 30% hydrogen peroxide solution, Merck), followed by 1 h boiling in 0.1 M sulfuric acid (diluted from 38% sulfuric acid, Sigma Aldrich) and 3 times boiling for 1 h in milli-Q water. Before and after each boiling step, the membranes were washed with milli-Q water. Finally, the membranes were dried in a flow of nitrogen followed by 10 min of drying in an oven at 100 °C. Each membrane was then hot-pressed at 2 MPa and 135 °C for 60 s. Thereafter, the membrane and the anode were pressed together at 2 MPa and 135 °C for 60 s, and finally, the anode-membrane-cathode assembly was pressed at 2 MPa and 135 °C for 60 s. During fuel cell operation, the fuel cell temperature was varied between room temperature and 90 °C with measurements taken at 25 °C, 30 °C, 40 °C, 50 °C, 60 °C, 70 °C, 80 °C, and 90 °C. The H_2/Ar flow rate was 50 ml min^{-1} and an over-stoichiometric O_2 flow rate of 50 ml min^{-1} was used. The gases were humidified to 100% relative humidity, and the cell was operated without backpressure. The presented data of the measurements have not been iR-corrected. The scan rate for the polarization curve measurements was 10 mV s^{-1}. Potentiostatic electrochemical impedance spectroscopy (EIS) analysis was done to assess cell resistance via the high frequency resistance (HFR) intercepts. Measurements were done at room temperature and 0.6 V vs. RHE between 100 kHz and 0.01 kHz with 10 measurement points per decade. Experiments to assess the stability of the catalyst in relation to MEA preparation procedure were done potentiostatically at 0.3 V vs. RHE with measurement points collected every 20 s. All electrochemical experiments were done using a Gamry Reference 600 potentiostat. The polarization curves presented in this study are collected after a pre-conditioning procedure in which the fuel cell is run through 60-70 potentiodynamic cycles between −0.3 V vs. RHE and open circuit potential (OCP) at 10 mV s^{-1}. During this pre-conditioning procedure, the polarization curves stabilize and become repeatable. However, some of the prepared MEAs, namely, those prepared by air brush, resulted in relatively unstable fuel cell performances. For these MEAs, data from the first measured cycle are presented instead.

In order to optimize the performance of a MEA using this new type of Fe/N-OMC cathode catalyst material, several preparation parameters needed to be optimized. More specifically, we found the Nafion to catalyst ratio, the catalyst loading in the MEA, the sonication time of the catalyst Nafion mixture to form the catalyst ink as well as the method with which the ink was applied to the GDL to be important variables. These parameters depend on each other and cannot be optimized independently, which necessitate a time-intensive iterative approach to optimize them all. This part of the study was performed in several pre-studies to the presented work. Here, the final results of parameter optimization are shown, where only one parameter at a time is varied and its influence discussed, while the other parameters are held at optimized values. During all optimization experiments, the best performances of the catalyst were reached in the temperature interval between 60 °C and 80 °C. At temperatures of 90 °C, the fuel cell performance decreased, although the performance was recovered once the temperature was lowered again. This indicates that the catalyst and MEA do not degrade at 90 °C. The performance decrease is therefore likely due to water management issues of the used PEMFC setup at high temperatures and thus independent from the used MEA.

Effect of the catalyst ink application procedure. By far the most influential parameter of MEA preparation turned out to be the procedure used to apply the catalyst ink to the GDL. Apparently, the speed with which the catalyst ink is applied greatly affects the overall performance of the MEA in the fuel cell. Generally, the catalyst ink was applied by pipette to the GDL, and the best results were achieved when applying the catalyst ink under conditions where fast evaporation of the lower aliphatic alcohol-based solvent used in the catalyst ink was achieved. More specifically, the cathodes prepared at elevated temperatures performed better, regarding both activity and stability, than cathodes prepared at room temperature. Polarization curves of these MEAs illustrating their activity performance are shown in Fig. 1. Preparation temperatures of 35-40 °C were found to be optimal for the catalyst ink used. At temperatures above 40 °C, large visible cracks formed in the applied catalyst layer, which lead to delamination of the catalyst from the GDL thus reducing the active area. It should be noted that the activity loss due to delamination is not proportional to the delaminated area but smaller than the lost active area would have suggested. This indicates that preparation temperatures above 40 °C might result in even better catalyst performance provided the formation of cracks and subsequent delamination can be avoided. In an attempt to reduce crack

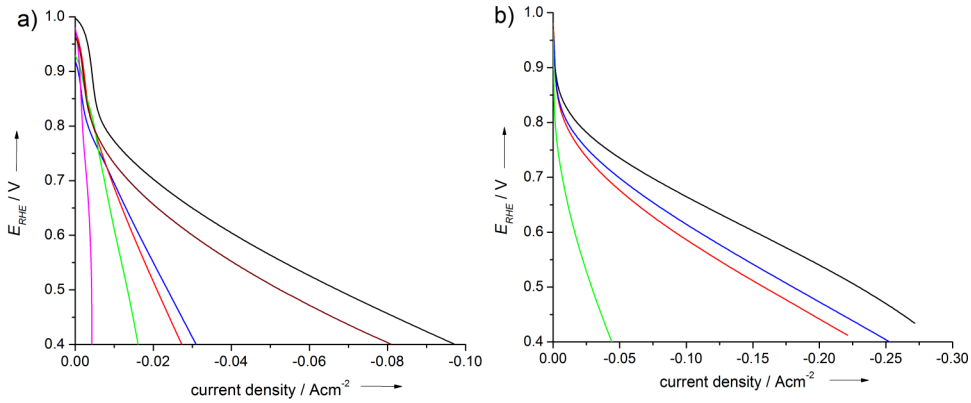

FIG. 1. Polarization curves of differently prepared cathodes measured at 60 °C. Preparation with pipette at 40 °C (black), with pipette at RT (blue), with air brush at 40 °C (green), and a procedure where the catalyst was grinded with Nafion before pipette application at 40 °C (red). Image (a) shows polarization curves using an as-synthesized Fe/N-OMC catalyst, while (b) shows the same measurement using an acid-washed and heat-treated Fe/N-OMC catalyst. In (a), an oxygen free reference measurement (magenta) and an electrode prepared with a pipette at 40 °C without thorough grinding (brown) are included.

formation and delamination of the active layer, cathodes were fabricated by applying the catalyst ink using an air brush instead of pipette, since, in principle, the air brush allows for electrodes with very homogenous active layers with minor delamination or surface cracks. However, the MEAs prepared at 40 °C using air brush instead of pipette achieved low activities as shown in Fig. 1 and were, in addition, not catalytically stable but degraded fast over time. This held true both when using the as-synthesised catalyst powder (Fig. 1(a)) and acid-washed catalyst powder (Fig. 1(b)), the acid-washing being a procedure used to improve catalyst performance described elsewhere.[23]

The lower performance of cathodes prepared at room temperature or by using air brush does not origin from delamination since this was not a problem observed for these electrodes. Instead, we hypothesise that their lower performance is due to that Nafion covers too much of the catalyst surface. For the electrodes prepared at room temperature, this could, in principle, be caused by the slower solvent evaporation allowing Nafion to diffuse longer in the catalyst pores. This would result in the catalyst surface being covered by Nafion to a higher degree than for samples prepared at higher temperature, where a more rapid evaporation of the solvent occurs, thus limiting Nafion diffusion. A similar explanation is proposed for the reduced performance of the cathodes prepared by air brush. Here, catalyst ink is sprayed on the GDL in a slow layer-by-layer process which could allow for the Nafion to diffuse longer in the catalyst pores thus covering a larger percentage of the catalyst surface area. If the Nafion coverage on the catalyst is indeed what limits the performance of the electrodes prepared at room temperature or by air brush, an electrode specifically prepared with a high Nafion coverage should exhibit low activity and stability performance. To test this hypothesis, an electrode was prepared by extensively mixing the catalyst powder with Nafion, where the mixing was done not only by sonication but additionally by a mechanical mixing step with mortar and pestle. This extended mixing results in an increased coverage of the catalyst by Nafion. We find that the electrodes prepared using the catalyst powder extensively mixed with Nafion exhibit poor activity (Fig. 1) and also low stability of the active layer in the fuel cell. The observed activity decrease in these MEAs is consistent with the hypothesis of excess Nafion on the catalyst particles. The activity decrease can be explained by increased electrical resistance due to restricted current flow caused by non-conducting Nafion blocking connections between catalyst particles and the GDL or, alternatively, due to the absence of 3-phase boundaries. The observed stability issues can, in accordance with the hypothesis, be caused by accelerated carbon degradation due to electrochemical corrosion. This carbon degradation is expected to occur as a consequence of the reduced number of available pathways for electrical conduction when most carbon is covered by Nafion. The few remaining pathways become bottlenecks and the currents passing through these become higher, which lead to increased corrosion in these areas. Additionally, corrosion is known to increase carbon hydrophilicity,[27] which leads to decreased gas permeability due to water

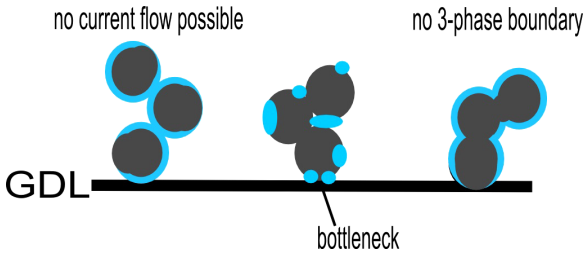

FIG. 2. Schematic cross-sectioned image of catalyst particles (grey) with excess coverage of Nafion (blue). Three effects are illustrated: no paths available for current flow, formation of bottlenecks with high current densities, and absence of the necessary 3-phase boundary.

accumulation in the carbon pores. Fig. 2 illustrates the proposed issues schematically illustrating three possible characteristics of excess Nafion in the electrode.

An indication which of the three proposed characteristics in Fig. 2 dominates can be obtained by EIS analysis. In Fig. 3, EIS measurements using an optimized cathode, a room-temperature dried cathode, a cathode with an extensively mixed catalyst, and a cathode prepared by air brush are compared. All cathodes were freshly prepared and EIS measurements were conducted after conditioning by scanning 10 cycles between OCP and 0.1 V vs. RHE at 50 mV/s. The ohmic cell resistances determined at the HFR intercepts using these cathodes are 166 mΩ cm^{-2} in the optimized case, 200 mΩ cm^{-2} for the room-temperature dried cathode, 253 mΩ cm^{-2} when using the extensively mixed catalyst, and 697 mΩ cm^{-2} for the air brushed cathode. These ohmic resistances are in correlation to the activity of the corresponding cathodes shown in the polarization curves in Fig. 1(b). Specifically, the high resistance measured for the air brush prepared cathode is likely what limits the performance of this electrode. Apparently, the excess Nafion results in drastically reduced current flow between different catalyst agglomerates. The results are consistent with a slow layer-by-layer catalyst deposition scenario in which each layer produced by the air brush deposits on the GDL as a separate unit with Nafion covering most of the outer catalyst surface as well as penetrating the catalyst pores, resulting in a deposit with poor conductivity between catalyst particles and with corresponding impaired current flow. The slow layer-by-layer deposition does not occur in the case of catalyst ink deposition by pipette. However, it seems that if the solvent in the catalyst ink evaporates slowly, as is the case with the room temperature dried electrode, Nafion can diffuse longer to more efficiently cover the catalyst surface and pores, and penetrate in between catalyst particles. This again leads to poor conductivity due to the separation of different catalyst particles by Nafion and thus reduces the possible flow of current. A similar effect is likely occurring if the catalyst is extensively grinded with Nafion, which again allows for the Nafion to accumulate between catalyst particles. It can be concluded that some cathode

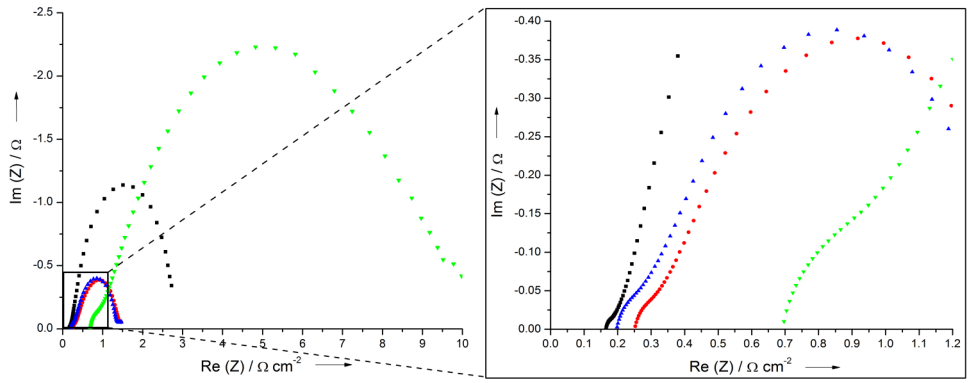

FIG. 3. Nyquist plot of the EIS measurements at room temperature and 0.6 V vs. E_{RHE} using an optimized cathode (black—square), a cathode dried at room temperature (blue—triangle upwards), a cathode prepared from an extensively mixed Nafion catalyst ink (red—round), and a cathode prepared using an air brush (green—triangle downwards).

preparation techniques lead to too large Nafion coverage of the catalyst resulting in high electronic resistance in the electrode, the characteristics of which can be illuminated by EIS. One should also note that the ink application procedure not only affects the ohmic resistance but also the charge transfer resistance. Observing the EIS spectra of the freshly prepared cathode in Fig. 3, it seems that cathodes prepared at room temperature and by grinding with Nafion exhibit lower charge transfer resistance than the optimised cathode. This, however, only is the case while the cathodes are fresh. The not optimised cathodes degrade fast (Fig. 9) leading to a significant increase in charge transfer resistance (see supplementary material for EIS spectra of degraded cathodes). The charge transfer resistance is inversely proportional to the exchange current density. The exchange current density in turn depends heavily on the physical properties of the cathode, like surface roughness. This strengthens our claim that a not optimized ink application procedure leads to corrosion and possibly even disintegration of the catalyst.

Effect of grinding the catalyst powders. An additional highly important parameter for the MEA preparation is the influence of pre-grinding of the dry, as-synthesised catalyst powder. This is illustrated in Fig. 1 where the thoroughly grinded catalyst performs significantly better than the same catalyst used without pre-grinding. We found this improvement to be a general phenomenon and fuel cell measurements of all our as-synthesized catalysts showed only a low activity for the ORR, while grinded catalysts generally performed significantly better. Mechanical grinding does not change the nano- or mesostrucutre thus the positive effect of grinding must originate from changes in the larger microstructure of the catalyst. To better understand the mechanism of this improvement, the surface conformation of the as-synthesised catalysts was imaged by SEM. In the SEM images shown in Fig. 4, a thin non-porous layer was observed to cover the catalyst surface. This layer likely consists of un-templated carbon residues formed during the synthesis. Because of its non-porous nature, the layer will block access to the porous interior of the catalyst material underneath and thus limit access to the active sites, consequently lowering the overall oxygen reduction efficiency of the catalyst.

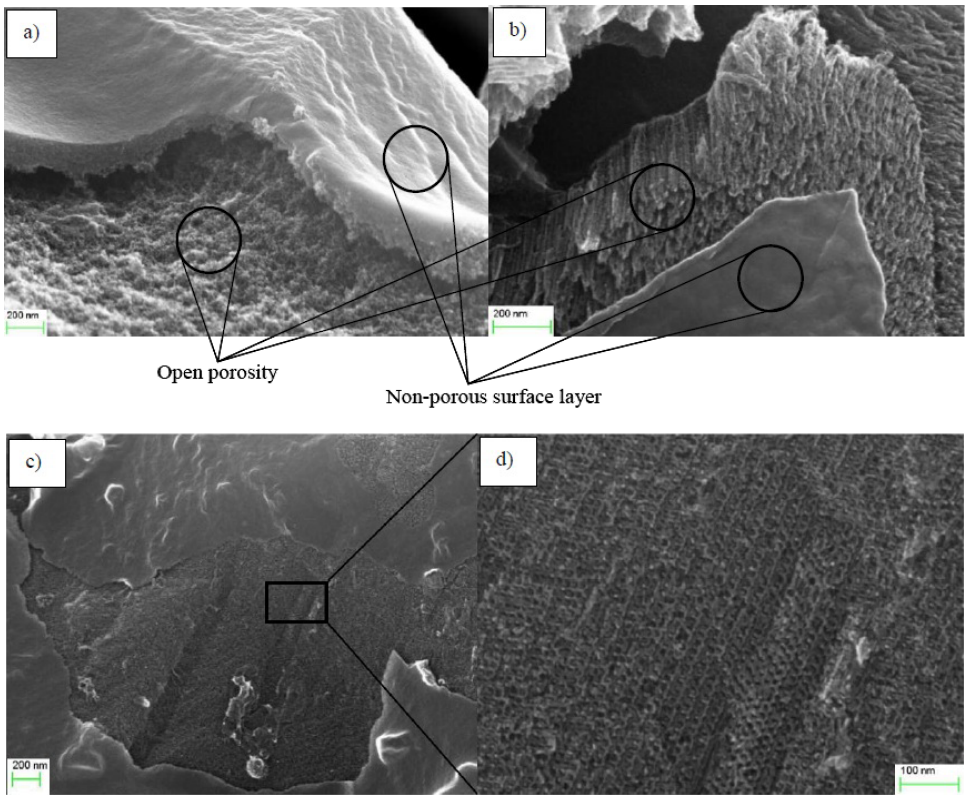

FIG. 4. SEM images of the as-synthesized Fe/N-OMC catalyst pyrolized at 950 °C ((a) and (b)) and a Fe/N-OMC catalyst pyrolized at 1100 °C ((c) and (d)). The acceleration voltage used was 10 kV.

By gently grinding the catalyst powder, its meso-order remains largely unaffected, while the particles' size decreases resulting in a specific surface area increase (see supplementary material for specific surface area measurements). This observation can be rationalised by the uncovering of fresh catalyst surface underneath the non-porous layer upon grinding. This allows then for improved access of the reactants to the active sites and for better water transport out of the catalyst layer, which explains the observed improvement in catalytic performance of the ground catalysts. Hence, from here on, all catalysts were ground to fine powders before preparing the catalyst ink.

Influence of the catalyst ink sonication time. The duration of the interaction between the catalyst powder and the Nafion in solution during cathode preparation has great influence on the activity and stability performance of the prepared MEA. This is not only true for the time spent on applying the catalyst ink on the GDL, as discussed above in the section on the effect of the catalyst ink application procedure, but also when the catalyst ink was left standing for an extended time (>1 h) before applying it to the GDL or when the catalyst ink was sonicated for a longer time (>20 min). In consequence, the catalyst ink used for MEA preparation was not stored, and the sonication time for the ink preparation was optimized. A time window of 5-20 min was found ideal for sonication of the catalyst ink. At both longer and shorter sonication times, a performance decrease particularly at high currents of the cathode could be observed as illustrated in Fig. 5(a). This is attributed to very low Nafion coverage of the catalyst in the case of sonication times below 5 min and too high Nafion coverage of the catalyst in the case of sonication times above 20 min. A typical catalyst ink used in this study was therefore sonicated for 15 min. This clear time dependence was not observed in the purely activity controlled region (Fig. 5(b)) indicating that sonication mainly has an effect on the mass transport properties of the catalyst/ionomer material but not on its inherent activity.

Effect of the ionomer to catalyst ratio. The next optimization parameter of importance is the ionomer (here Nafion) to catalyst ratio used when preparing the catalyst ink. This parameter has recently been optimized for other noble metal-free catalysts[28,29] but not for the particular case of functionalized OMC structures. In Fig. 6, fuel cell polarization plots obtained from catalyst inks with Nafion loadings of 33 wt. %, 37.5 wt. %, 41 wt. %, 45 wt. %, and 50 wt. % are shown. It is notable that no Nafion loading is optimal in the entire observed potential region. At low currents and potentials around 0.8 V vs. RHE, a Nafion loading of 41 wt. % seems to be ideal (Fig. 6(b)). Loadings of 37.5 wt. % and 45 wt. % also result in good performance in the low current region, while performance of the cathodes loaded with 33 wt. % and 50 wt. % was 2-3 times worse than for an optimized cathode (Fig. 6(b)). A change is observed at 0.67 V vs. RHE. Between 0.67 V vs. RHE and 0.4 V vs. RHE, the cathode with 37.5 wt. % performs the best. This changes again in the completely mass transport limited low potential high current range where the cathode with only 33 wt. % Nafion performs the best (Fig. 6(a)). It thus appears that in the low current range, high

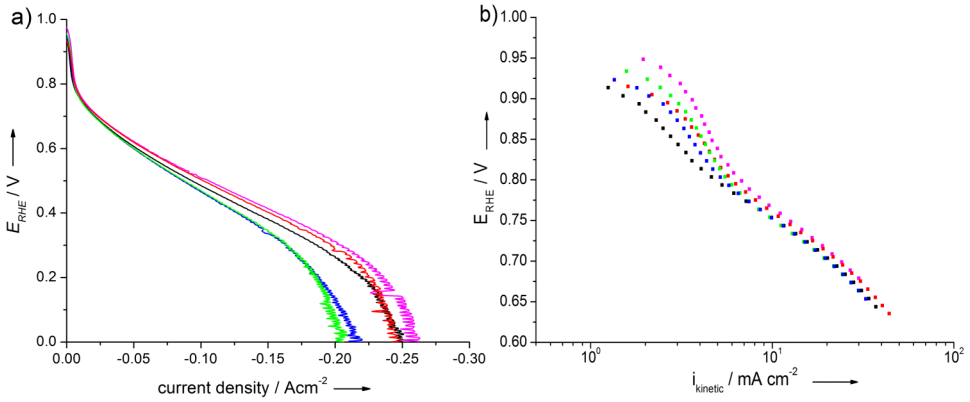

FIG. 5. Fuel cell performance using catalyst inks prepared from Fe/N-OMC sonicated for different periods of time (green—30 s, red—5 min, magenta—20 min, black—1 h, blue—4 h). The catalyst loading used was 8 mg cm^{-2} and the measurements were done at 80 °C. (a) Shows the polarization curves and (b) the Tafel plot in the high voltage region most relevant to fuel cell operation.

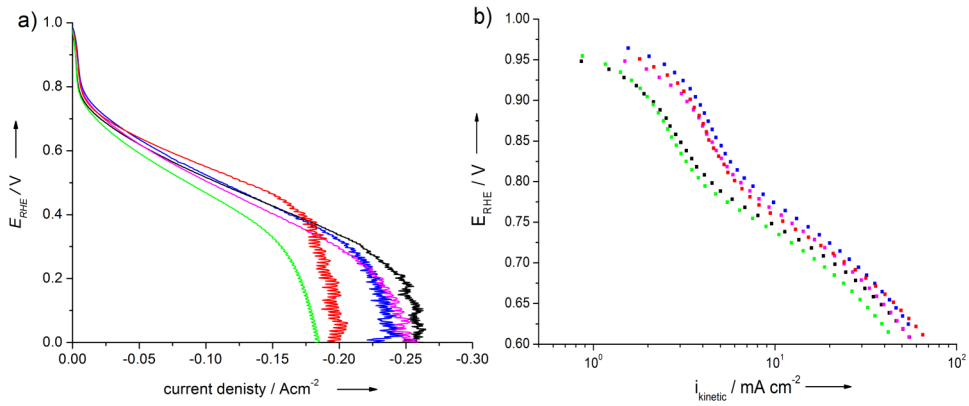

FIG. 6. Fuel cell measurements using catalysts with varying Nafion to catalyst ratio performed at 80 °C using a Fe/N-OMC catalyst with a specific surface area of 800 m^2 g^{-1}. (a) Shows the polarization curves and (b) the Tafel plot in the high voltage region most relevant to fuel cell operation. Nafion concentrations used were: 50 wt. % (green), 45 wt. % (magenta), 41 wt. % (blue), 37.5 wt. % (red), and 33 wt. % (black).

Nafion content is beneficial as it allows for the formation of many three phase boundaries. However, too high Nafion content leads to a performance decrease, as can be seen in the cathode with 50 wt. % Nafion in Fig. 6, probably due to a decrease in gas phase boundary area. In the high current region on the other hand, a lower Nafion content in the electrode seems to be favourable, which is attributed to the fact that high Nafion content can lead to concentration over-potentials caused by the accumulation of water at the active sites. This water accumulation is caused by the increased interaction between water and the partly hydrophilic Nafion at high currents.[30]

As a general result for all tested catalysts, a ratio of 41 wt. % Nafion to 59 wt. % catalyst was found optimal for the activity-controlled potential region between OCP and 0.67 V vs. RHE. This Nafion to catalyst ratio proved to be optimal independently if the catalyst was functionalized by iron or cobalt as long as the specific surface area of the catalyst was between 600 and 900 m^2 g^{-1}. The Nafion to catalyst ratio we report here is slightly higher than the ratios reported to be suitable for many conventional Pt catalysts, where a Nafion loading of 33 wt. % or lower is considered optimal.[30–32] The need for a higher Nafion loading for our functionalized OMC catalysts is attributed to their larger specific surface area. However, the ideal catalyst to Nafion ratio found here is lower than that reported for other noble metal-free catalysts.[28,29] This is attributed to the functionalized OMCs higher wettability for Nafion compared to the carbon blacks usually used as support materials for noble metal-free catalysts.

Optimization of the catalyst loading on the cathode. The final parameter optimized in this study is the catalyst loading on the cathode. This parameter has a major influence on the overall fuel cell performance. Generally, the performance increases with higher catalyst loading due to the increased number of active sites. If that would be the only effect, a linear dependence between catalyst loading and performance is expected. This is, however, not the case since thicker catalyst layers lead to mass transport restrictions as well as higher iR-resistance in the MEA. In Fig. 7, the influence of catalyst loading on fuel cell current output and ohmic resistance is shown for Fe/N-OMC catalysts. Fig. 7(a) additionally shows the current output performance of a Co/N-OMC catalyst with respect to the catalyst loading on the cathode. From these data, an ideal catalyst loading was found to be 6-8 mg cm^{-2} as a compromise between a large number of active sites and reasonable mass transport restrictions.

MEA preparation for catalysts synthesised under different conditions. The optimization procedures discussed this far were performed using the same batch of Fe/N-OMC catalyst. We have found, however, that these optimized values are also valid for functionalized OMC catalyst materials synthesised under different conditions and with different elemental compositions. The pyrolysis reaction can, for example, be performed in the range from 700 °C to 1100 °C without having to change the MEA preparation procedures. A similar non-porous surface layer as discussed for the catalyst pyrolized at 950 °C is also observed for catalysts pyrolized at 1100 °C (see Figs. 4(c) and 4(d)).

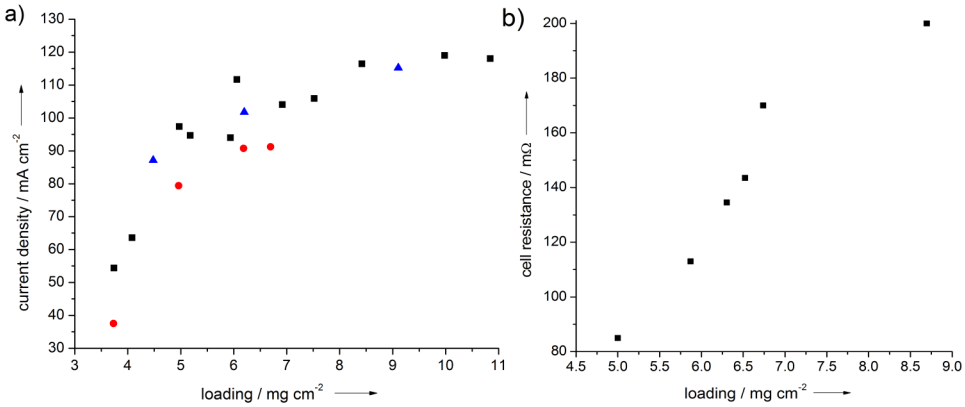

FIG. 7. Influence of catalyst loading on (a) the current output of the fuel cell and (b) on ohmic cell resistance. Catalyst loading data include the Fe/N-OMC catalyst (black—square), a second Fe/N-OMC catalyst pyrolized at 1100 °C (blue—triangle), and a catalyst containing Co instead of Fe (red—round).

Similarly, the current dependency on catalyst loading using a catalyst synthesised at 1100 °C follows the same trend as the catalyst prepared at 950 °C (Fig. 7—blue triangles). Even OMC catalysts functionalized with cobalt instead of iron exhibit a similar dependence (Fig. 7—red circles). The only instance where an adjustment of the optimized MEA preparation parameters becomes necessary is when preparing MEAs using very high surface area functionalized OMC catalysts. Such catalysts can be synthesised by impregnating the template only once by precursor solution and not twice as described in the experimental part. This procedure results in functionalized OMC catalysts with specific surface areas larger than 900 $m^2\ g^{-1}$. This results in the need for 1-5 wt. % more Nafion in the catalyst ink than for a corresponding catalyst ink containing a catalyst with lower surface area in order to reach an optimal performance.

Influence of the MEA preparation on durability. This far, the discussion of the MEA performance has been focused on catalyst activity; in the following section, the influence of the MEA preparation procedure on the MEA durability will be discussed. As mentioned earlier, in this study, the duration of some of the MEA preparation steps, mainly the catalyst ink sonication step and the method of application of catalyst ink on the GDL play a major role in the final MEA performance. From these observations, one might think that the functionalized OMC catalysts are very unstable on the GDL, but that is not the case. Instead, once the solvent on the electrode has evaporated at a suitable temperature and Nafion has been immobilized, the electrode proves to be stable during storage. It can be measured in the fuel cell directly after preparation or after being stored in ambient conditions for several weeks without any detectable difference in performance. Also, once the electrode is part of a MEA, the MEA can be stored for weeks and even be used, then stored for weeks and then again used without a decrease in activity due to storage. This stability is illustrated in Fig. 8, where a MEA was run for 15 h, then stored for 3 weeks and finally run for another 75 h. In fact, after storage, the MEA even showed a temporary increase of activity rather than a decrease.

Concerning the influence of the MEA preparation parameters on durability, several effects were observed. In Fig. 9, the time-dependence of the fuel cell performance of MEAs prepared with different procedures is shown. The black and orange curves were measured on MEAs prepared with optimized parameters as discussed above. The orange curve was measured at 0 V vs. RHE, meaning physically the measured current is the short circuit current. The fact that no degradation is seen when measuring at 0 V proves that the degradation effects on the observed timescale are mainly potential-related effects rather than connected to the current or external influences caused by the measurement setup such as fluctuations in temperature or humidity. The black curve was measured at 0.3 V vs. RHE and exhibits good stability not only in the 90 h long measurements used for comparing different MEA preparation procedures but also during a 525 h long degradation experiment shown in the inset in Fig. 9. Here, it is interesting to note that the interrupt points marked in the

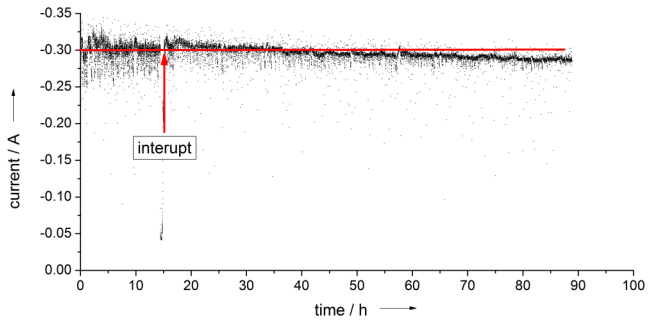

FIG. 8. Performance of a Fe/N-OMC catalyzed fuel cell during operation for 90 h at 80 °C and 0.3 V vs. RHE. After 15 h of continuous operation, the cell was shut down and the MEA stored for 3 weeks and subsequently used continuously for the remaining 75 h.

inset correspond to refills of the humidifiers in the fuel cell setup. The performance drop connected to these refills indicates the strong influence of cell water management on performance.

The red curve measured at 0.3 V vs. RHE origins from a MEA prepared with a catalyst loading twice as high as the optimal value. The initial activity of this MEA is lower than in the optimized case. This initial activity difference decreases somewhat during the degradation measurement, suggesting that the MEA with higher catalyst loading is slightly more stable than the one prepared with less catalyst. The fact that the MEA with higher catalyst loading does not show an optimal initial performance but better degradation behaviour than an optimized MEA agrees with the results presented above in the section on the effect of the ionomer to catalyst ratio. These results show that higher catalyst loading and the consequential thicker catalyst layer lead to increased current resistance and thus less activity but not to changes in the structural composition of the cathode. A very different behaviour is observed for MEAs prepared with catalyst ink-sonication times deviating from the optimized values. In Fig. 9, these MEAs are represented by the blue curve for 1 h sonication and the light green curve for 30 s sonication. For both curves, a fast degradation is observed. The situation is worse for the 30 s sonicated catalyst ink than for the 1 h sonicated ink and is presumably closely connected to the too high or too low coverage of the catalyst with Nafion

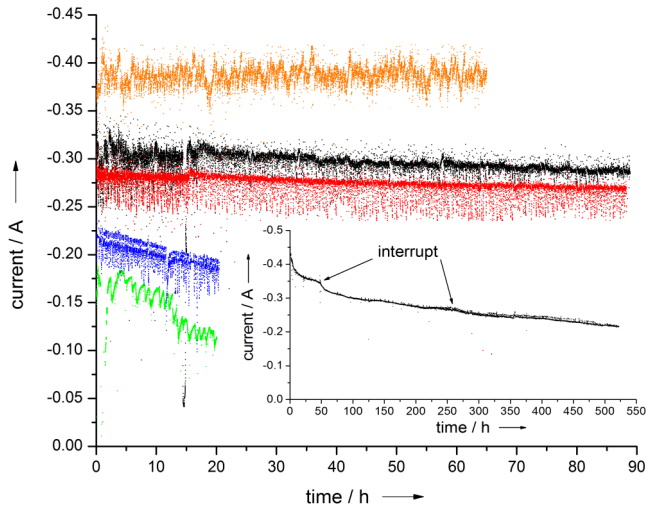

FIG. 9. Illustration of the degradation behavior of MEAs prepared with optimized (black) and not optimized MEA preparation parameters (15 mg cm^{-2} catalyst loading—red; 1 h sonication—blue; 30 s sonication—green). The fuel cell was operated at 70 °C and 0.3 V vs. RHE. For reference, an optimized MEA was measured at 0 V vs. RHE (orange). The inset shows performance of an optimized MEA over a period of 525 h during which the measurement was interrupted twice for humidifier refills.

as discussed previously. This observation also is consistent with the observations regarding the air brush fabricated cathode, and the cathode in which the catalyst was ground with Nafion discussed above in the section on the effect of the catalyst ink application procedure, as the MEAs with those cathodes degraded rapidly in less than an hour once employed in the PEMFC.

In conclusion, we can say that several important parameters for MEA preparation using transition metal ion-chelated ordered mesoporous carbon as cathode catalysts have been identified and optimized. It was found that grinding of the synthesised catalysts significantly improved the performance as a result of increasing the accessible surface area of the catalysts. The ideal catalyst loading on a cathode was found to be 6-8 mg cm^{-2} with a catalyst:Nafion ratio of around 41:59 by weight. Nafion seems to possess a high wettability for functionalized ordered mesoporous carbon materials. In consequence, there is an optimum time for mixing the Nafion solution with the catalyst powder in order to avoid covering the catalyst to a too high degree with Nafion thus reducing the amount of three phase boundaries or impeding the electrical current flow in the electrode. This makes fast application, for example, by pipette, of the catalyst ink on the GDL necessary. A cathode preparation temperature of 35-40 °C was found to be optimal while the optimal sonication time for the catalyst ink was found to be 5-20 min. The prepared cathodes and MEAs can be stored at ambient conditions for several weeks without exhibiting any degradation effects. It could further be shown that most variations in the synthesis of the transition metal functionalized OMC catalyst powders do not necessitate changes of MEA optimization parameters, indicating that the found parameters are applicable for a wide range of transition metal functionalized OMC catalysts. Additionally, the MEAs prepared using optimized parameters show promising durability during fuel cell operation while rapid degradation is observed for MEAs prepared outside the window of optimization. This illustrates the importance and applicability of the presented optimization parameters for both activity and stability performance.

The Swedish Research Council (VR) is gratefully acknowledged for project funding and a Senior Researcher grant for AECP.

[1] G. S. Tasic, S. S. Miljanic, M. P. M. Kaninski, D. P. Saponjic, and V. M. Nikolic, Electrochem. Commun. **11**, 2097 (2009).
[2] G. Wu, K. L. More, C. M. Johnston, and P. Zelenay, Science **332**, 443 (2011).
[3] M. Lefèvre, E. Proietti, F. Jaouen, and J.-P. Dodelet, Science **324**, 71 (2009).
[4] E. Proietti, F. Jaouen, M. Lefèvre, N. Larouche, J. Tian, J. Herranz, and J.-P. Dodelet, Nat. Commun. **2**, 416 (2011).
[5] Z. Chen, D. Higgins, A. Yu, L. Zhang, and J. Zhang, Energy Environ. Sci. **4**, 3167 (2011).
[6] C. W. B. Bezerra, L. Zhang, K. C. Lee, H. S. Liu, A. L. B. Marques, E. P. Marques, H. J. Wang, and J. J. Zhang, Electrochim. Acta **53**, 4937 (2008).
[7] C. W. B. Bezerra, L. Zhang, H. S. Liu, K. C. Lee, A. L. B. Marques, E. P. Marques, H. J. Wang, and J. J. Zhang, J. Power Sources **173**, 891 (2007).
[8] R. Bashyam and P. Zelenay, Nature **443**, 63 (2006).
[9] F. Jaouen, F. Charreteur, and J. P. Dodelet, J. Electrochem. Soc. **153**, A689 (2006).
[10] F. Jaouen, E. Proietti, M. Lefevre, R. Chenitz, J.-P. Dodelet, G. Wu, H. T. Chung, C. M. Johnston, and P. Zelenay, Energy Environ. Sci. **4**, 114 (2011).
[11] L. Zhang, J. J. Zhang, D. P. Wilkinson, and H. J. Wang, J. Power Sources **156**, 171 (2006).
[12] R. Othman, A. L. Dicks, and Z. Zhu, Int. J. Hydrogen Energy **37**, 357 (2012).
[13] V. Mehta and J. S. Cooper, J. Power Sources **114**, 32 (2003).
[14] M. Kim, J.-N. Park, H. Kim, S. Song, and W.-H. Lee, J. Power Sources **163**, 93 (2006).
[15] F. Charreteur, F. Jaouen, S. Ruggeri, and J.-P. Dodelet, Electrochim. Acta **53**, 2925 (2008).
[16] F. Charreteur, S. Ruggeri, F. Jaouen, and J. P. Dodelet, Electrochim. Acta **53**, 6881 (2008).
[17] P. V. Shanahan, L. Xu, C. Liang, M. Waje, S. Dai, and Y. S. Yan, J. Power Sources **185**, 423 (2008).
[18] E. Antolini, Appl. Catal., B **88**, 1 (2009).
[19] S. H. Joo, S. J. Choi, I. Oh, J. Kwak, Z. Liu, O. Terasaki, and R. Ryoo, Nature **412**, 169 (2001).
[20] S. H. Joo, C. Pak, D. J. You, S.-A. Lee, H. I. Lee, J. M. Kim, H. Chang, and D. Seung, Electrochim. Acta **52**, 1618 (2006).
[21] K. Wikander, H. Ekström, A. E. C. Palmqvist, A. Lundblad, K. Holmberg, and G. Lindbergh, Fuel Cells **6**, 21 (2006).
[22] K. Kwon, Y. J. Sa, J. Y. Cheon, and S. H. Joo, Langmuir **28**, 991 (2011).
[23] J. K. Dombrovskis, H. Y. Jeong, K. Fossum, O. Terasaki, and A. E. C. Palmqvist, Chem. Mater. **25**, 856 (2013).
[24] D. von Deak, E. J. Biddinger, K. A. Luthman, and U. S. Ozkan, Carbon **48**, 3637 (2010).
[25] D.-S. Yang, D. Bhattacharjya, S. Inamdar, J. Park, and J.-S. Yu, J. Am. Chem. Soc. **134**, 16127 (2012).
[26] F. Kleitz, S. H. Choi, and R. Ryoo, Chem. Commun. **2003**, 2136.
[27] R. Borup, J. Meyers, B. Pivovar, Y. S. Kim, R. Mukundan, N. Garland, D. Myers, M. Wilson, F. Garzon, D. Wood, P. Zelenay, K. More, K. Stroh, T. Zawodzinski, J. Boncella, J. E. McGrath, M. Inaba, K. Miyatake, M. Hori, K. Ota, Z. Ogumi, S. Miyata, A. Nishikata, Z. Siroma, Y. Uchimoto, K. Yasuda, K. I. Kimijima, and N. Iwashita, Chem. Rev. **107**, 3904 (2007).
[28] K. Artyushkova, D. Habel-Rodriguez, T. S. Olson, and P. Atanassov, J. Power Sources **226**, 112 (2013).
[29] F. Jaouen, V. Goellner, M. Lefèvre, J. Herranz, E. Proietti, and J. P. Dodelet, Electrochim. Acta **87**, 619 (2013).

[30] C.-Y. Ahn, J.-Y. Cheon, S.-H. Joo, and J. Kim, J. Power Sources **222**, 477 (2013).
[31] T. Frey and M. Linardi, Electrochim. Acta **50**, 99 (2004).
[32] S. Litster and G. McLean, J. Power Sources **130**, 61 (2004).
[33] See supplementary materials at http://dx.doi.org/10.1063/1.4902995 for results and experimental details, EIS spectra of degraded cathodes, specific surface area measurements, nitrogen physisorption, small angle X-ray scattering, and additional EIS data.